

This article was downloaded by: [IRSTEA]

On: 14 April 2015, At: 07: 17

Publisher: Taylor & Francis

Informa Ltd Registered in England and Wales Registered Number: 1072954

Registered office: Mortimer House, 37-41 Mortimer Street, London W1T 3JH, UK



Aerosol Science and Technology

Publication details, including instructions for authors and subscription information:

<http://www.tandfonline.com/loi/uast20>

Simulation of Aerosol Deposition in Granular Media

Yongwon Jung^a & Chi Tien^a

^a Department of Chemical Engineering and Materials Science, Syracuse University, Syracuse, NY, 13244

Published online: 11 Jun 2007.

To cite this article: Yongwon Jung & Chi Tien (1993) Simulation of Aerosol Deposition in Granular Media, *Aerosol Science and Technology*, 18:4, 418-440, DOI: [10.1080/02786829308959614](https://doi.org/10.1080/02786829308959614)

To link to this article: <http://dx.doi.org/10.1080/02786829308959614>

PLEASE SCROLL DOWN FOR ARTICLE

Taylor & Francis makes every effort to ensure the accuracy of all the information (the "Content") contained in the publications on our platform. However, Taylor & Francis, our agents, and our licensors make no representations or warranties whatsoever as to the accuracy, completeness, or suitability for any purpose of the Content. Any opinions and views expressed in this publication are the opinions and views of the authors, and are not the views of or endorsed by Taylor & Francis. The accuracy of the Content should not be relied upon and should be independently verified with primary sources of information. Taylor and Francis shall not be liable for any losses, actions, claims, proceedings, demands, costs, expenses, damages, and other liabilities whatsoever or howsoever caused arising directly or indirectly in connection with, in relation to or arising out of the use of the Content.

This article may be used for research, teaching, and private study purposes. Any substantial or systematic reproduction, redistribution, reselling, loan, sub-licensing, systematic supply, or distribution in any form to anyone is expressly forbidden. Terms & Conditions of access and use can be found at <http://www.tandfonline.com/page/terms-and-conditions>

Simulation of Aerosol Deposition in Granular Media

Yongwon Jung* and Chi Tien[‡]

*Department of Chemical Engineering and Materials Science,
Syracuse University, Syracuse, NY 13244*

A computer simulation method was developed for and applied in the study of aerosol deposition in granular media. A modified Happel model was used to characterize the structure of granular media. Based on comparisons with available experimental data, an empirical correction factor, the capture probability that ac-

counts for the various complications arising from the presence of particle deposits on the media, was established. By combining the use of this correction factor together with the simulation method, accurate prediction of aerosol collection in granular media with significant deposition can be made.

INTRODUCTION

Aerosol deposition in granular media is a complex and multifaceted phenomenon. With the flow of an aerosol suspension through a granular medium, some of the aerosols are deposited on the surface of the grains constituting the medium. The accumulation of deposited aerosols within the medium causes a continuing change in the medium structure, giving rise to the transient behavior of granular filtration, which shows an increase of collection efficiency and a decrease in permeability as the filter medium becomes clogged.

For an understanding of the problem of aerosol deposition, knowledge about the formation and growth of particle deposits under the influence of a number of forces is required. Such information is difficult to obtain experimentally because the structure of granular media consists of tightly compacted granular substances.

The use of two-dimensional filters (Ushiki and Tien, 1985; Yoshida and Tien, 1985) to observe aerosol deposition in situ was supposed to overcome this difficulty; however, it is difficult to extend observations from two-dimensional model filters to actual media which are three-dimensional.

A more practical way of obtaining detailed information on aerosol deposition in granular media is through a computer simulation that creates particle deposition from suspensions flowing past collectors of appropriate geometry. The articles by Tien et al. (1977) and Wang et al. (1977) postulate the basic principle of the deposition process on the premise that deposition may be viewed as the interplay of two effects: (a) the singular and random behavior of aerosol particles and (b) the shadow effect of deposited particles.

The principle of Tien et al. and Wang et al. was subsequently adopted by a number of investigators. Kanaoka et al. (1980), Ho (1981), Tsiang et al. (1982), and Ramarao and Tien (1988) applied this technique to analyzing aerosol deposition in fibrous media. The work of Kanaoka et al. dealt with diffusive aerosols. For

*Present address: Environmental Engineering Lab., Korea Atomic Energy Research Institute, P.O. Box 7, Daeduk-Danji, Taejeon, 305-606, Korea.

[‡]To whom correspondence should be addressed.

diffusive aerosols, particle trajectories are not deterministic. Consequently, traditional trajectory analysis for determining collection efficiencies is not applicable. Instead, Kanoaka et al. used the simulation technique for estimating the initial collection efficiencies. This approach was subsequently adopted by Gupta and Peters (1985) in their work of deposition on isolated spheres.

Another application of the simulation method is its use in examining the effect of deposition on collection efficiencies, the feasibility of which was demonstrated by both Beizaie et al. (1981) and Pendse and Tien (1982). Application of the simulation method to obtain deposition results under practical conditions, however, has not yet been done because of the excessive computational requirement.

In the present study, we extend and refine the previous simulation studies and develop a more efficient method than those proposed before so that particle deposition in granular media may be simulated under practical conditions. In addition, an empirical correction factor was introduced in order to account for a variety of effects such as the bouncing-off of impacting particles and the change of the flow field around collectors when the extent of deposition becomes significant.

PRINCIPLE OF SIMULATION

Simulation of aerosol deposition may be carried out based on the premises proposed by Tien et al. (1977) and Wang et al. (1977) previously. The procedure of simulation is composed of the following steps:

1. Selection of a model for granular media characterization,
2. Generation of particle trajectories,
3. Determination of adhesion of impacting particles,
4. Inventory of deposited particles.

In sum, simulation yields the results of the number of particles deposited as a function of the number of particles flowing past (or through) a collector as well as the positions of the deposited particles. The later information gives the morphology of deposited particles. The former results can be used to determine directly the unit collector efficiency defined as

$$\eta = \frac{dN}{dM} \quad (1)$$

where N is the number of the deposited particles and M is the number of particles flowing past the collector.

SELECTION OF POROUS MEDIA MODEL

To begin simulation, one must first select a granular media model. For a reasonable prediction of aerosol deposition rates, it is obvious that an acceptable model must adequately describe the flow field within the medium. At the same time, the model must be sufficiently simple so that its use in simulation is practical.

Among the several models that have been used for aerosol filtration studies, only the dense cubic packing model has been found to give good results on deposition rates (Gal et al., 1985). The structure of this model and its flow field expressions are, however, too complex to be used in simulation. In contrast, for the simpler models, neither the Happel nor the constricted-tube model was found to give reasonable results as pointed out by Paretzky et al. (1971) and Pense et al. (1978).

The failure of Happel's model in predicting correct collection efficiency is attributed to the underestimation of the jetting effects of fluid flow in porous media (Snaddon and Dietz, 1980). To correct this shortcoming, Vaidyanathan (1989) and Vaidyanathan et al. (1989) modified Happel's model by considering the entry of fluid into Happel's cell as

being through a window of a given size, which may be characterized by the angle, 2β , over which the window extends instead of the entire half sphere of the cell. (See Figure 1 for a schematic representation.) Furthermore, Vaidyanathan et al. assumed that granular media may be represented by a collection of such cells with the window sizes following a certain distribution function. Although this idea was found useful in improving the accuracy of predicting hydrosol deposition, its use in simulation is nevertheless impractical because of its excessive computational demand.

As an alternative to Vaidyanathan's modification, it was assumed in this study that the windows for all the cells have the same size. The window size was determined by carrying out a trajectory calculations using different window sizes and comparing the calculated collection efficiencies with experiments. It was found that a window of about 20° in size gives reasonably good agreement with experiments. This modification was then used in this simulation study.

DETERMINATION OF PARTICLE TRAJECTORIES

According to the assumption of Tien et al. (1977), aerosol particles enter into a Happel cell one at a time and are randomly distributed over the window. Trajectories of aerosols may be determined by integrating the particle equations of motion with the knowledge of the initial particle velocities and positions.

Assignment of Initial Positions

The initial positions of the succeeding entering particles over the window at the fluid envelope may be given by the spheri-

cal polar coordinates (R_b, θ, ϕ) . For any position (R_b, θ, ϕ) , $0 \leq \theta \leq \beta$ ($\beta = \pi/2$) and $0 \leq \phi \leq 2\pi$, the probability of the particle's center being within an area element over the window is proportional to the volumetric flow rate through the element. Thus, one has

$$\text{probability}(0 \leq \theta \leq \beta) = 1 \quad (2)$$

$$\text{probability}(0 \leq \phi \leq 2\pi) = 1 \quad (3)$$

$$G_1(\theta) = \text{probability}(\theta_{\text{in}} \leq \theta) = \frac{\sin^2\theta}{\sin^2(\pi/9)} \quad (4)$$

$$G_2(\phi) = \text{probability}(\phi_{\text{in}} \leq \phi) = \phi/2\pi \quad (5)$$

From the cumulative probability density functions, $G_1(\theta)$ and $G_2(\phi)$, of random variables θ_{in} and ϕ_{in} , respectively, one can find these random variables by using the two uncorrelated random numbers R_1 and R_2 distributed uniformly over $(0, 1)$ as follows:

$$\theta_{\text{in}} = G_1^{-1}(R_1) = \sin^{-1}(\sqrt{R_1} \sin \beta) \quad (6)$$

$$\phi_{\text{in}} = G_2^{-1}(R_2) = 2\pi R_2 \quad (7)$$

A random number generator, RAN 1 (Press et al., 1987), was used in this study to generate sets of R_1 and R_2 .

Particle Trajectory Equations

Assuming that inertial, viscous drag, and gravitational forces are the only forces acting on a particle in motion¹ and, furthermore, that particle motion in ϕ direc-

¹In other words, the mechanisms of particle deposition and inertial impaction, sedimentation, and interception.

tion is absent, the equations of particle motion for the coordinate system shown in Figure 1 are given as

$$N_{st} \frac{d^2 r^*}{dt^{*2}} + \frac{dr^*}{dt^*} - N_{st} r^* \left(\frac{d\theta}{dt^*} \right)^2 - \nu_r^* + N_G \cos \theta = 0 \tag{8}$$

$$N_{st} \frac{d^2 \theta}{dt^{*2}} + \frac{d\theta}{dt^*} + \frac{2N_{st}}{r^*} \frac{dr^*}{dt^*} \frac{d\theta}{dt^*} - \frac{\nu_\theta^*}{r^*} - N_G \frac{\sin \theta}{r^*} = 0 \tag{9}$$

$$\phi = \phi$$

where r^* , θ , and ϕ are the dimensionless coordinates of the position of the particle center and t^* is the dimensionless time. r^* , t^* as well as the other quantities pres-

ent in Eqs. 8 and 9 are defined as:

$$R_c = d_g/2 \tag{10a}$$

$$r^* = r/R_c \tag{10b}$$

$$t^* = tV_s/R_c \tag{10c}$$

$$\nu_\theta^* = \nu_\theta/V_s \tag{10d}$$

$$\nu_r^* = \nu_r/V_s \tag{10e}$$

$$N_{St} = \rho_p d_p^2 V_s / (9\mu d_g) \tag{10f}$$

$$N_G = (\rho_p - \rho)gd_p \tag{10g}$$

where t is the time and r is the radial coordinate. ν_r and ν_θ are the particle velocity components along the r and θ directions, and ν_s is the gas approach velocity. R_c is the collector (filter grain) radius. N_G and N_{St} are the gravitational and Stokes parameters. Besides ν_s , the quantities used in defining these two parameters include the particle and grain diameters d_p and d_g , the particle and gas densities ρ_p and ρ , the gas viscosity μ , and the gravitational acceleration.

The fluid velocity components (dimensionless) ν_r^* and ν_θ^* can be found from the flow-field expression for the modified Happel model (Vaidyanathan, 1989) if the change in flow field due to particle deposit is negligible. The expressions of ν_r^* and ν_θ^* are given in the Appendix.

The initial conditions are

$$r^* = b \quad \theta = \theta_{in} \quad \phi = \phi_{in} \tag{11a}$$

$$\nu_r^* = -\alpha \cos \theta \quad \text{at } t = 0 \tag{11b}$$

$$\nu_\theta^* = \alpha \sin \theta \tag{11c}$$

where α is flow intensification factor defined as (Vaidyanathan, 1989)

$$\alpha = 2/(1 - \cos 2\beta) \tag{12}$$

Thus, by specifying its initial condition, one can determine the trajectory of a particle by integrating Eqs. 8 and 9. This procedure, however, is impractical because of the very large number of particle trajectories to be determined in a simula-

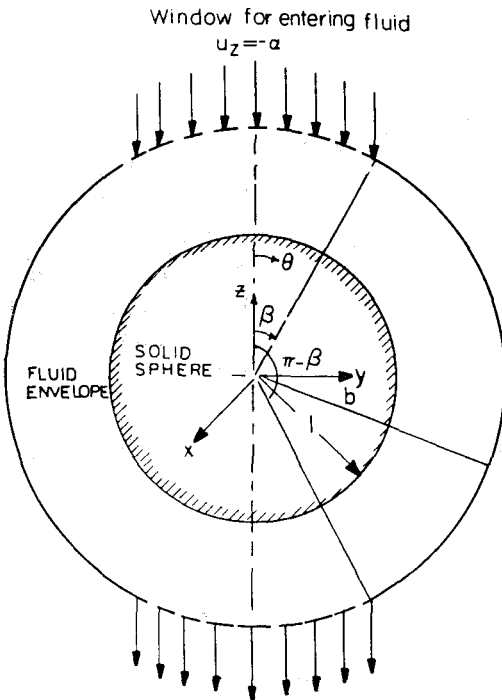


FIGURE 1. Modified Happel's model.

tion. Instead, only a small number of particle trajectories corresponding to specified positions of entry were determined by integrating Eqs. 8 and 9. Particle trajectories with entering positions other than the specified ones may be estimated by an interpolation procedure described below.

Estimation of Particle Trajectories by Interpolation

Because of the axisymmetry of the flow field, the trajectory of a particle can be described by the r coordinate of the particle's position as a function of the corresponding θ coordinate and its initial θ coordinate value, or, $r^*(\theta_{in}, \theta)$. Based on this feature, an interpolation method was developed as follows. First, N_p discrete positions of entry at the window of the modified Happel cell (namely, at θ_i for $i = 1, 2, \dots, N_p$ with $\theta_{N_p} = \pi/9$) were specified. For a particle entering at θ_i , the r coordinate of its trajectory could be expected to be greater than θ_i . Its trajectory, therefore, may be described by a set of $M_p - i$ discrete values of $r^*(\theta_{in} = \theta_i, \theta_j)$ with $j = i, i + 1, \dots, M_p$, $M_p = \pi/2$. This set of r values were then obtained from integrating Eqs. 8 and 9 with the initial position being $r^* = b$, and $\theta = \theta_i$. In other words, for a given set of values of θ_i , the trajectory meshes which can be used in the interpolation scheme were created.

For any particle with entry position other than those specified, for example, with $\theta_i < \theta_{in} < \theta_{i+1}$, the radial position of the particle at θ_j , $j = i + 1, i + 2, \dots, M_p$, were approximated by the following linear interpolation formula

$$\begin{aligned}
 r^*(\theta_{in}, \theta_j) &= r^*(\theta_i, \theta_j) \\
 &+ \left[\frac{r^*(\theta_{i+1}, \theta_j) - r^*(\theta_i, \theta_j)}{\Delta \theta_i} \right] \\
 &\times (\theta - \theta_i)
 \end{aligned} \tag{13}$$

where

$$\Delta \theta_i = \theta_{i+1} - \theta_i \tag{14}$$

$$r^*(\theta_i, \theta_i) = R_b/R_c = b \tag{15}$$

Similarly, the radial position of the particle at any given θ , with $\theta_j < \theta < \theta_{j+1}$, approximated as

$$\begin{aligned}
 r^*(\theta_{in}, \theta) &= r^*(\theta_{in}, \theta_j) \\
 &+ \left[\frac{r^*(\theta_{in}, \theta_{j+1}) - r^*(\theta_{in}, \theta_j)}{\Delta \theta_j} \right] \\
 &\times (\theta - \theta_j)
 \end{aligned} \tag{16}$$

where

$$\Delta \theta_j = \theta_{j+1} - \theta_j \quad j = i + 1, i + 2, \dots, M_p \tag{17}$$

To reduce the interpolation error, finer meshes were used in the region near the axis of symmetry, where the curvature of streamlines changes rapidly than those used in the region away from the axis of symmetry. Specifically, for the region $\theta \leq 1^\circ$ the angular increment, $\Delta \theta_i$, was taken to be 0.1° . For the region $1^\circ < \theta \leq 20^\circ$, $\Delta \theta_i$ was 0.25° ; i.e.,

$$\text{for } \theta \leq 1^\circ \quad \Delta \theta_i = 0.1^\circ \quad \Delta \theta_j = 0.1^\circ \tag{18a}$$

$$\text{for } 1^\circ < \theta \leq 20^\circ \quad \Delta \theta_i = 0.25^\circ \quad \Delta \theta_j = 0.25^\circ \tag{18b}$$

$$\text{for } 20^\circ < \theta \leq 90^\circ \quad \Delta \theta_j = 0.25^\circ \tag{18c}$$

For particles entering the region with its θ coordinate $< 0.1^\circ$, their trajectories were determined directly by integrating

Eqs. 8 and 9 with the initial conditions given by Eq. 11.

A similar interpolation procedure was used to estimate particle velocities.

DETERMINATION OF THE OUTCOME OF AN APPROACHING PARTICLE

There are three possible outcomes for any particle approaching the collector:

1. Deposition on the collector surface,
2. Deposition on a previously deposited particle, or
3. Escape from collection.

An approaching particle escapes collection if the following conditions are satisfied by its trajectory:

$$r^*(\theta, \phi) > 1 + N_R \quad (19a)$$

and

$$d_i > 2N_R \quad \text{for all } i \quad (19b)$$

where d_i is the distance (nondimensionalized in terms of the radius of a collector) between the center of the particle and the center of i th deposited particle.

The requirements for a particle to be deposited are: (a) the particle has to make contact with either a collector or any one of the previously deposited particles, and (b) there must be a sufficiently strong attractive force such that, once the particle makes contact with the collector or any previously deposited particles, adhesion occurs.

To determine whether or not the first condition is satisfied, the particle's trajectory must be compared with the positions representing the collector surface as well as the surface of all previously deposited particles. In principle, this is accomplished by incrementing the θ coordinate in steps of $\Delta\theta_t$ along the particle trajectory, checking whether either one of the two relations, Eqs. 19a and 19b, is not

satisfied. Checking in this manner, however, requires excessive computer time. To reduce the time requirement, the following scheme was devised:

1. The entire upper half region of the modified Happel cell is discretized along the θ and ϕ coordinates, depicted in Figure 2. The size of a grid in the direction of ϕ was 4° while the size of a grid in the direction of θ was made exactly the same as that of trajectory meshes as stated before. Accordingly, the positions of deposited particles are identified in terms of a three-dimensional grid system where they are located, as well as by the order of their deposition in the grid. In other words, the particles in each grid have their own identification numbers according to their order of deposition in the grid. For example, for the n th deposited particle in the grid (k, j) , one can store the position of the particle by using a three-dimensional array [i.e., $X(n, k, j)$, $Y(n, k, j)$ and $Z(n, k, j)$]. In this way, one can first identify the likely region of particle deposition by locating the grid with deposited particles, thereby significantly reducing computer time.
2. For a grid with no deposited particles, it is obvious that the possibility of an approaching particle's being deposited inside this grid is nil. Thus, the only possibility to be checked is that of an approaching particle's being deposited on the collector surface as it passes through the empty grid.
3. Furthermore, in each and every grid the highest radial-coordinate position of a deposited particle is monitored and updated as the simulation progresses. Accordingly, if the radial position of an approaching particle in a grid is much higher than the highest radial position of deposited particles in the grid, particle deposition cannot take

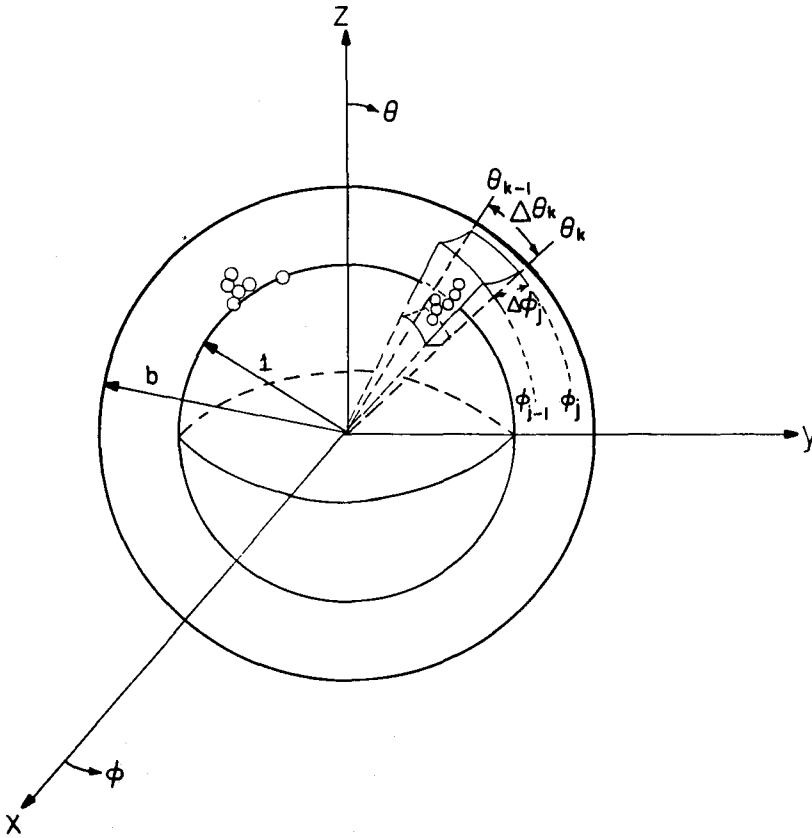


FIGURE 2. The grid system used for recording deposited particles.

place in the grid, and the particle will move to the next grid.

4. If deposited particles are present in a grid, and the approaching particle does not make contact with the collector while the particle is within the grid, then the particle is first returned to one of its previous positions, and the distances between the approaching particle and all the previously deposited particles in the grid are calculated to see if particle deposition takes place on a previously deposited particle. This calculation continues while the particle moves forward.
5. For an approaching particle located at a position close to the boundary be-

tween two adjacent grids in terms of ϕ , all the deposited particles in these two grids were included in the comparison, since the approaching particle may be deposited on either one of the deposited particles present in the two grids.

A more detailed description of the algorithm used in carrying out the checking process can be seen from the flow chart (Figure 3).

CRITERIA FOR DEPOSITION

Two criteria were considered for determining adhesion of impacting particles:

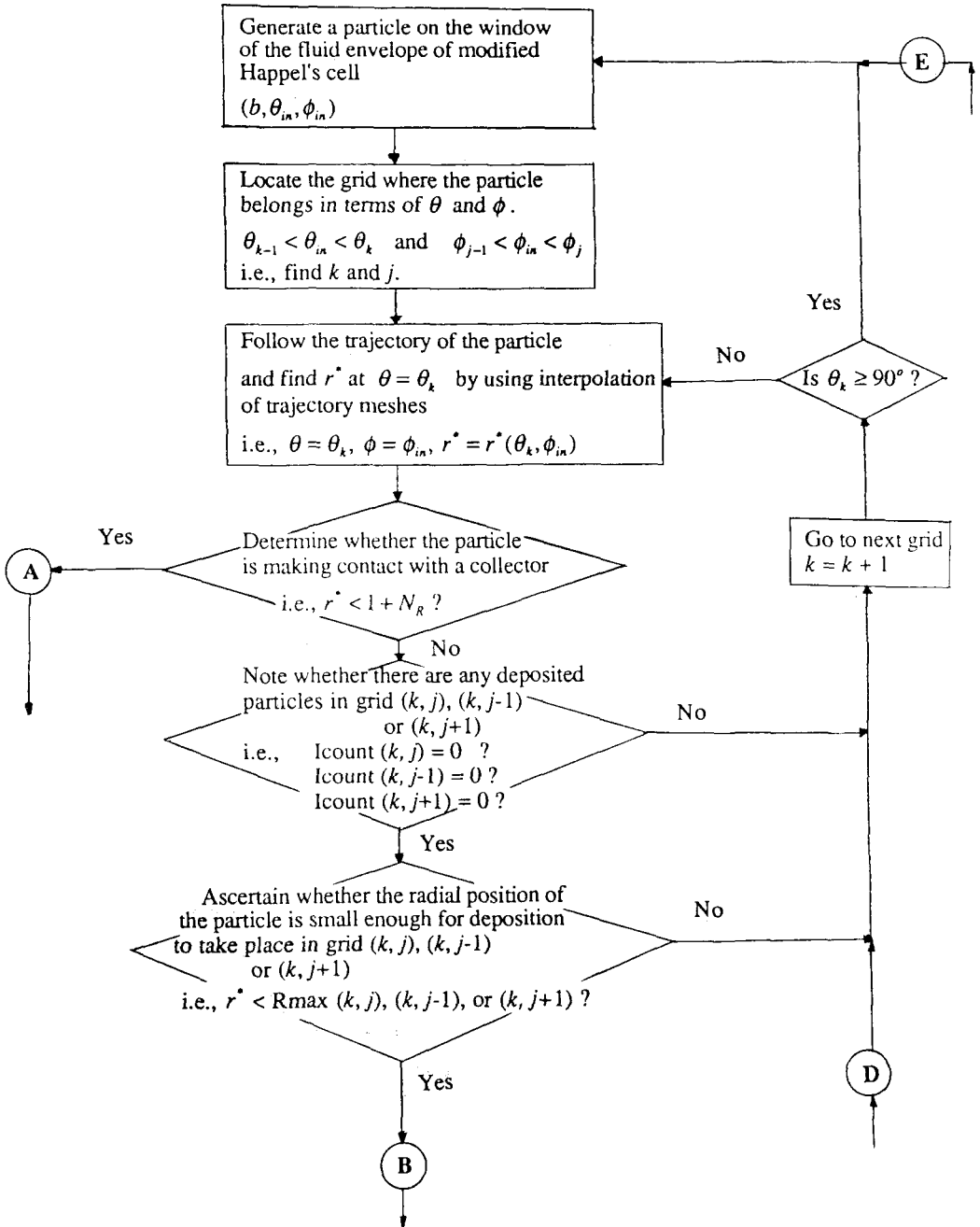


FIGURE 3. Flow charts for determining the adhesion of impacting particles.

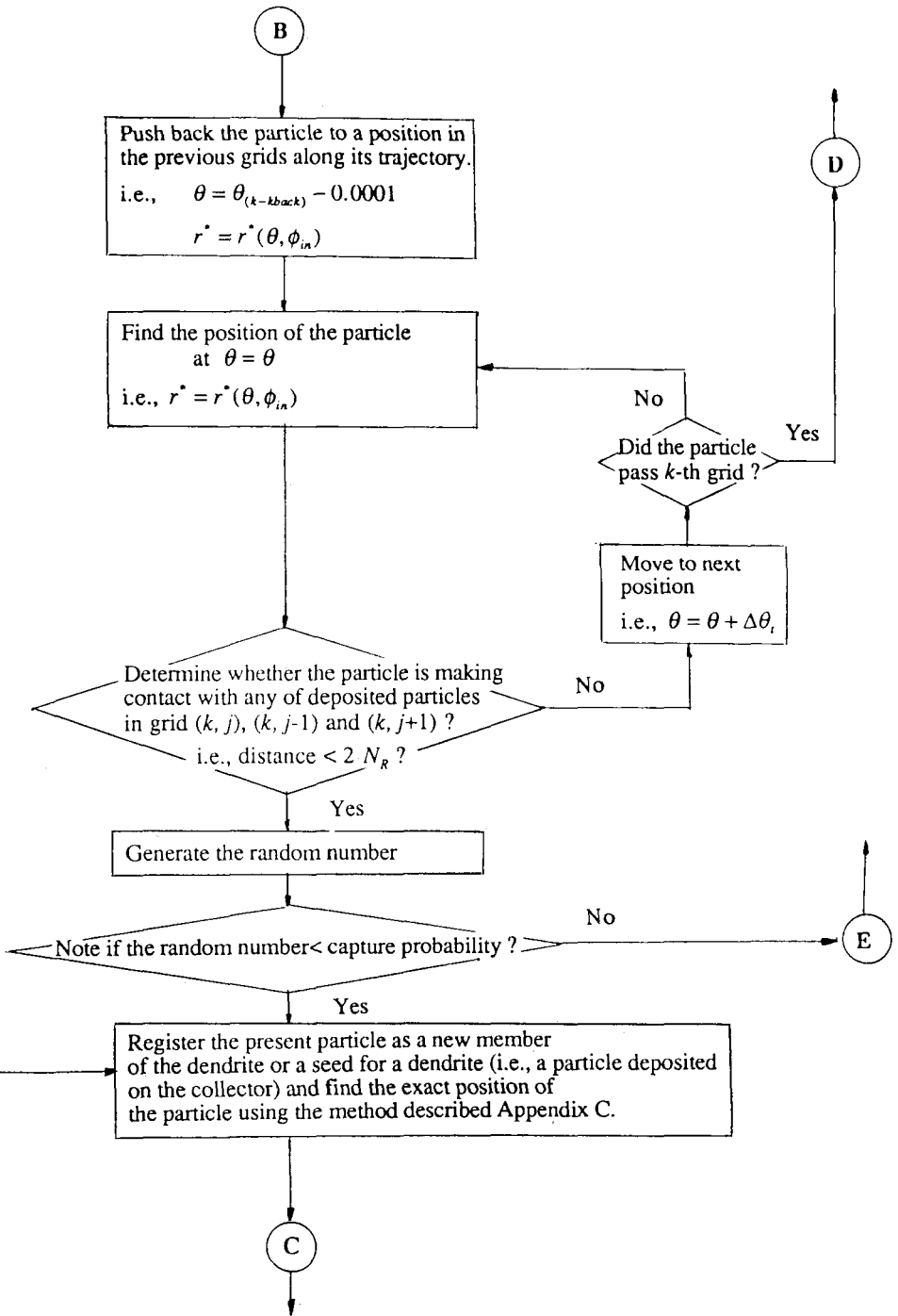
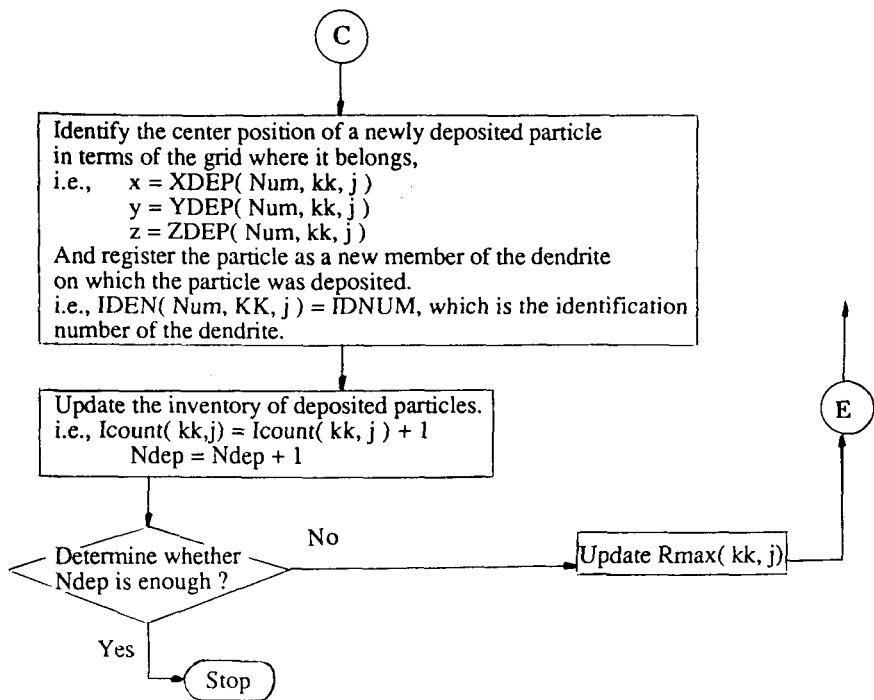


FIGURE 3. (Continued).



$XDEP(Num, kk, j) =$ the center position of the Num-th deposited particle in grid (kk, j) in terms of x .

$YDEP(Num, kk, j) =$ the center position of the Num-th deposited particle in grid (kk, j) in terms of y .

$ZDEP(Num, kk, j) =$ the center position of the Num-th deposited particle in grid (kk, j) in terms of z .

$Icount(kk, j) =$ the number of deposited particles in grid (kk, j) .

$Rmax(kk, j) =$ the highest position of the deposited particle in grid (kk, j) in terms of r, R_k , plus $3N_R$
(i.e., $Rmax(kk, j) = R_k + 3 N_R$)

$IDNUM =$ the identification numbers of dendrites

$IDEN(Num, kk, j) =$ the identification number of the dendrite where Num-th deposited particle in grid (kk, j) was deposited.

$Ndep =$ total number of deposited particles.

FIGURE 3. (Continued).

Particle Bounce-off

Dahneke (1972) stated that, when a particle collides with a surface, the bounce-off or adhesion of the particles onto the surface depends upon the magnitude of the particle's incident normal velocity being greater or less than the capture limit velocity, V_{esc} defined as

$$V_{\text{esc}} = \left[\frac{2\Delta E}{m} \frac{1 - e^2}{e^2} \right]^{1/2} \quad (20)$$

where ΔE is the particle-surface adhesion energy, m is the particle mass, and e is the coefficient of restitution defined as the ratio of the normal particle velocity at the instant of rebound to the normal particle velocity at the instant of contact.

As pointed out by Tsiang (1982), there are certain uncertainties in applying Eq. 20 for adhesion criterion. Dahneke (1972) showed that the elastic flattening of a sphere and/or indentation of a surface caused by the molecular attractions between the sphere and the surface molecules may cause a substantial increase in adhesion energy. The adhesion energy of flattened particles may be 20 times that of unflattened particles. Furthermore, when a particle collides with a previously deposited particle, accurate estimation of the particle velocity upon impact (in particular, the velocity normal to the previously deposited particle) is often difficult since particle trajectories were determined without considering the effect of deposition. These two problems make the use of the adhesion criterion questionable as shown in the later results.

Capture Probability

As an alternative to account for the various complications not considered in the simulation such as the change in flow field due to deposition, the bounce-off of impacting particles, and the possible hydro-

dynamic interaction effect, the capture probability was introduced in simulation as an empirical correction factor. It is defined as the probability of an approaching particle to be collected on a deposited particle or a collector when the approaching particle makes contact with the deposited particle or the collector based on the assumption that there is no change of flow field due to particle deposits and no hydrodynamic interaction between the approaching particles and the deposited particle (including the collector).

One can intuit the capture probability to be a function of a number of variables including d_p , V_s , N_{St} , and N_R as well as of the shape of particle clusters or dendrites. Also, it may be a function of the material constants of the impacting particle and the collector. Our objective, however, is pragmatic and is limited to determining an overall value such that the simulation results agree with experimental data. The justification for and success of this empirical approach, of course, are found in its ability to define such a parameter with consistency and generality. The incorporation of the capture probability in simulation was carried as follows: First, the value of the capture probability is selected arbitrarily. Next, the trajectory of an oncoming particle is monitored until the particle makes contact with either the collector or a previously deposited particle. If the particle makes contact with a collector, a uniform random deviate between 0 and 1 is generated. If the value of the random deviate is less than or equal to the assumed value of the capture probability, the particle is assumed to be deposited. On the basis of best agreement between experiments and prediction, a capture probability is determined empirically.

SIMULATION RESULTS

Two types of information, namely, the number of particles deposited, N , versus

the number of particles flowing past the collector, M , and the positions of deposited particles may be obtained from simulation. The second type of information gives the deposited morphology and its evolution with time. The unit collector efficiency can be found in the results of N vs. M according to Eq. 1.

The extent of particle deposition may be described by the specific deposit, σ , defined as the volume of deposited particles per unit medium value. In terms of N , σ may be written as

$$\sigma = N(1 - \epsilon)(d_p/d_g)^3 \quad (21)$$

where d_p and d_g are the diameter of the aerosol particle and packing grain, respectively.

The transient behavior of aerosol deposition in granular media is characterized by the changes in collection efficiency as the media becomes clogged. Quantitative relationship between η and σ is required for the rational design of granular filtration systems. A body of experimental data of η vs. σ have been collected in recent years (Takahashi et al., 1986; Walata et al., 1986; Jung, 1991; Jung and Tien, 1991). In the following, we compare our simulation results with the more recent data of Jung and Tien (1991). The conditions that were used in the experimental work are listed in Table 1, and the simulation was made using a super computer (IBM 3090-

600E at Cornell National Supercomputer Facility, Ithaca, NY).

Simulation without Considering the Effects of Flow Field Change, Hydrodynamic Interaction, and Bounce-off

As an initial attempt to compare simulation with experimental results, the simulation runs were made with the assumption that the flow-field change due to the presence of particle deposits, the hydrodynamic interaction between an approaching particle and previously deposited particles, and the bounce-off of particles upon impact with a previously deposited particle are absent (i.e., capture probability is 1.0). The conditions used in the simulation runs were the same as those used in experiments of Jung and Tien (1991) and are given in Table 1.

A typical comparison of the simulation and experimental results is shown in Figure 4. Although both sets of results indicate an increase in η with the increase in σ , they are not in good agreement. The degree of disagreement between them becomes pronounced as the extent of deposition increases. The collection efficiencies predicted by simulations are always greater than those obtained by experiments as specific deposit increases. Similar conclusions were also obtained by

TABLE 1. Conditions Used for Simulation

d_p (μm)	d_g (μm)	u_s (cm/s)	N_{St}	N_R	N_G
1.1	262	11.3	3.924×10^{-3}	4.198×10^{-3}	3.95×10^{-4}
1.1	262	15.8	5.491×10^{-3}	4.198×10^{-3}	1.53×10^{-4}
1.1	262	20.8	7.223×10^{-3}	4.198×10^{-3}	2.14×10^{-4}
1.1	525	11.3	1.958×10^{-3}	2.095×10^{-3}	3.95×10^{-4}
1.1	525	20.8	3.605×10^{-3}	2.095×10^{-3}	2.14×10^{-4}
1.1	525	31.8	5.504×10^{-3}	2.095×10^{-3}	1.41×10^{-4}
1.1	525	43.6	7.547×10^{-3}	2.095×10^{-3}	1.03×10^{-4}
2.02	525	11.3	6.219×10^{-3}	3.850×10^{-3}	6.81×10^{-4}

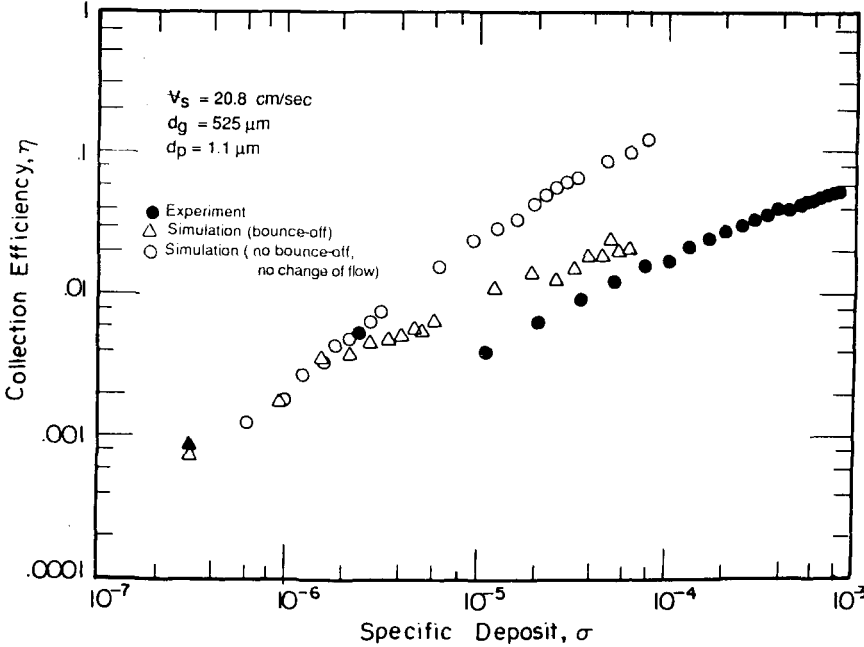


FIGURE 4. Comparisons between simulations and experiments—the effect of including particle bounce-off.

Tsiang et al. (1982) in their study of aerosol deposition in model fibrous filters.

Simulation Results Considering the Bounce-off of Impacting Particles

It can be expected that the difference between simulation and experiments shown in Figure 4 may be reduced by including the effect of bounce-off of impacting particles in simulation. The bounce-off of impacting particles can be determined by comparing the incident particle velocity (in normal direction) with the capture limit velocity V_{esc} defined by Eq. 20.

To determine V_{esc} , it was assumed that the adhesion energy, ΔE , is 10 times that given by the classical Bradley-Hamaker theory, as Tsiang assumed previously (Tsiang, 1980). According to the classical Bradley-Hamaker theory, the adhesion energy between two adhering particles of

diameter d_1 and d_2 is

$$\Delta E = \frac{Hd_1d_2}{12\delta_0(d_1 + d_2)} \quad (22)$$

$$= \frac{Hd_1}{24\delta_0} \text{ if } d_1 = d_2 \quad (23)$$

where H is the Hamaker constant and δ_0 is the separation distance between the particles. The value of δ_0 is not known exactly but is often estimated to be about 4 Å (Tien, 1989). By substituting Eq. 23 into Eq. 21, the capture-limit velocity are given as

$$V_{esc} = \frac{1}{d_1} \left[\frac{H(1 - e^2)}{2\pi\delta_0\rho_p e^2} \right]^{1/2} \quad (24)$$

The capture limit velocity can, therefore, be calculated if one knows the values of H , e , and δ_0 . The coefficient of restitution, e , is given as (Zener, 1941)

$$e = e_0 + \exp(-1.7\Lambda) - 1 \quad (25)$$

where e_0 is the thick-body value of e (i.e., no flexural work), which is estimated to be 0.95, and Λ is the inelasticity parameter defined as (Tien, 1989)

$$\Lambda = \frac{2}{3\pi^{2/5}} \left(\frac{d_p}{d_g} \right)^2 \left(\frac{1}{1 + d_p/d_g} \right)^{1/10} \times \left(\frac{V_{ni}}{V_c} \right)^{1/5} \left(\frac{\pi_p}{\pi_c} \right)^{3/5} \times \left(\frac{k_c}{k_p + k_c} \right)^{2/5} \quad (26)$$

where V_{ni} is the normal incident velocity of a particle and V_c is defined as $1/(k_p k_c)$. d_p and d_g are the particle and the collector diameters, and k_p and k_c are defined for the particle and collector materials, respectively, by $k_i = (1 - \bar{\nu}_i^2)/Y_i$, where $\bar{\nu}_i$ and Y_i are Poisson's ratio and Young's modulus for material i . If it is assumed that Eq. 26 can be applied to the case where two particles of the same sizes are colliding, then one has (Ramarao and Tien, 1988)

$$\Lambda = \frac{(2)^{1/2}}{3\pi^{2/5}} \left(\frac{V_{ni}}{V_c} \right)^{1/5} \quad (27)$$

The relevant physical constants for polyvinyltoluene latex particles are found to be (Tsiang, 1980)

$$\rho_p = 1.027 \text{ g/cm}^3$$

$$d_p = 1.1, 1.02 \text{ } \mu\text{m}$$

$$\bar{\nu}_p = 0.33$$

$$Y_p = 0.32 \times 10^{11} \text{ dyn/cm}^2$$

$$H = 1.0 \times 10^{-12} \text{ erg}$$

$$\delta_0 = 4 \text{ } \text{\AA}$$

The calculated values of capture limit velocities obtained by using these physical constants and the relevant equations are

$$V_{esc} = 30.51 \text{ cm/s for } 1.1 \text{ } \mu\text{m}$$

latex particles

$$V_{esc} = 15.75 \text{ cm/s for } 2.02 \text{ } \mu\text{m}$$

latex particles

The simulation results including the bounce-off effect are also shown in Figure 4. It is clear that, by including the bounce-off effect, agreement between simulation and predictions improves, but the difference nevertheless exists. The results also show that the effect of bounce-off is significant only at high values of σ .

The effect of deposition is generally manifested in the increase of η with the increase in σ as shown in Figure 4. However, with the bounce-off consideration, this monotonic increase in η with σ may no longer be valid. An example of this is shown in Figure 5, which gives the unit collector efficiency vs. σ for the deposition of 1.1- μm aerosol particles in media composed of glass spheres of diameter of 525 μm at a superficial velocity of 43.55 cm/s. With inclusion of the bounce-off effect, the simulation results show a decrease of η with σ when the specific deposit exceeds 6×10^{-5} .

Determination of Capture Probability

As shown in Figures 4 and 5, simulation results fail to agree with experiments regardless whether the bounce-off effect is included or not. Furthermore, the capture limit velocity that is used as the criterion for adhesion cannot be determined without uncertainty. Accordingly, a more pragmatic and direct alternative to account for the various complications not included in the simulation would be the use of an empirically determined corrected factor which we term the capture probability. Such an approach, of course, is arbitrary. However, if a consistent value of this correction factor can be found, the practical purpose of developing the simulation method can then be realized.

The determination of the capture probability can be illustrated by the example shown in Figure 6, which shows η vs. σ under the conditions similar to those of

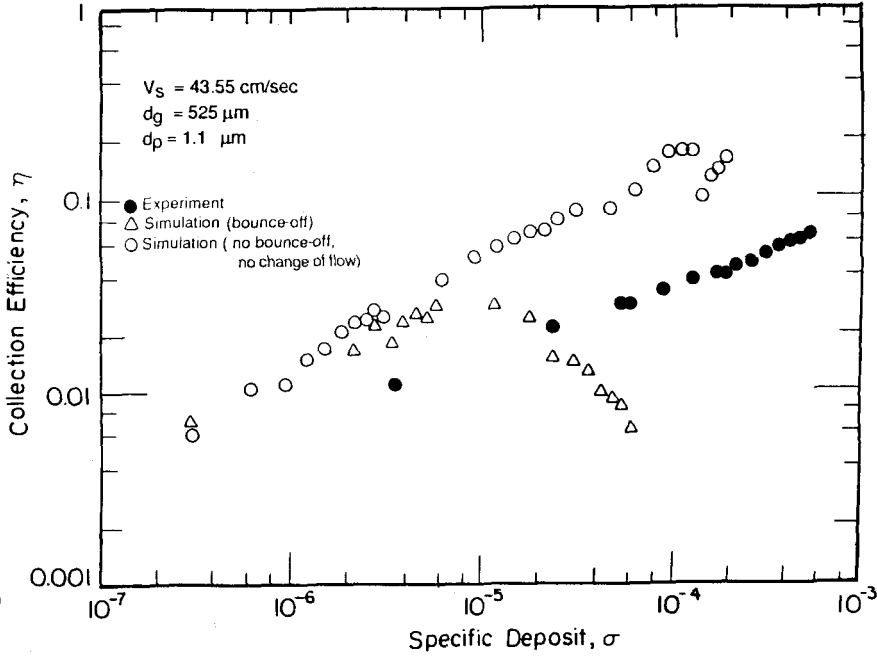


FIGURE 5. Comparisons between simulations and experiments—significant bounce-off causing a decline in η with the increase of σ .

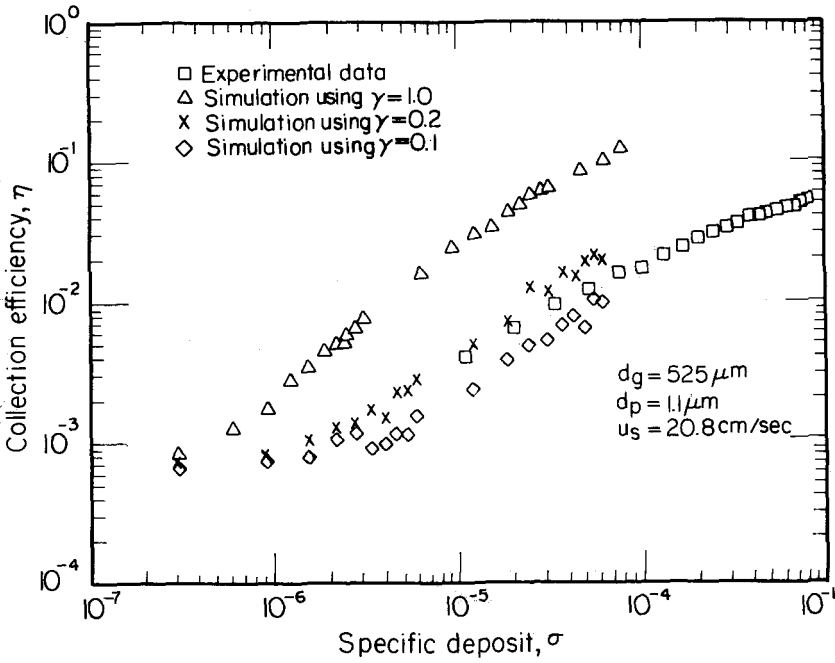


FIGURE 6. Effect of using capture probability on simulation.

Downloaded by [IRSTEIA] at 07:17 14 April 2015

Figure 4. The simulation results are those obtained with the capture probability, γ equal to 1.0, 0.2, and 0.1, respectively. It is obvious that η decreases as the capture probability decreases. For this case, the experimental data are bracketed by the simulation results corresponding to $\gamma = 0.1$ and $\gamma = 0.2$. By successive trial and error, it was found that the best agreement was obtained with $\gamma = 0.15$. Similar determinations under different simulation conditions were also made and the results are summarized in Table 2. The agreement between the simulation results incorporating the use of γ and experiments are shown in Figures 7 and 8. It is clear that with the use of this correction factor, good prediction of η vs. σ indeed can be made using the simulation method.

It should be noted that, although γ is an empirical factor and varies with a number of variables as shown by the results given in Table 2, the degree of change of γ is, however, relatively small (ranging from 0.15 to 0.23). In the absence of its

TABLE 2. Numerical Values of γ

d_p (μm)	d_g (cm)	u_s (cm/s)	$\bar{\gamma}$
1.1	262	11.1	0.2
1.1	262	15.81	0.21
1.1	262	20.8	0.23
1.1	525	11.3	0.15
1.1	525	20.8	0.15
1.1	525	31.76	0.18
1.1	525	43.55	0.2
2.02	525	11.3	0.14

precise values, an average value of γ based on those given in Table 2 may be used in the simulation.

Deposit Morphology

From the simulation results, one can also obtain information concerning the morphology of particle deposits, which varies with the extent of deposition and variables such as particle size, gas velocity,

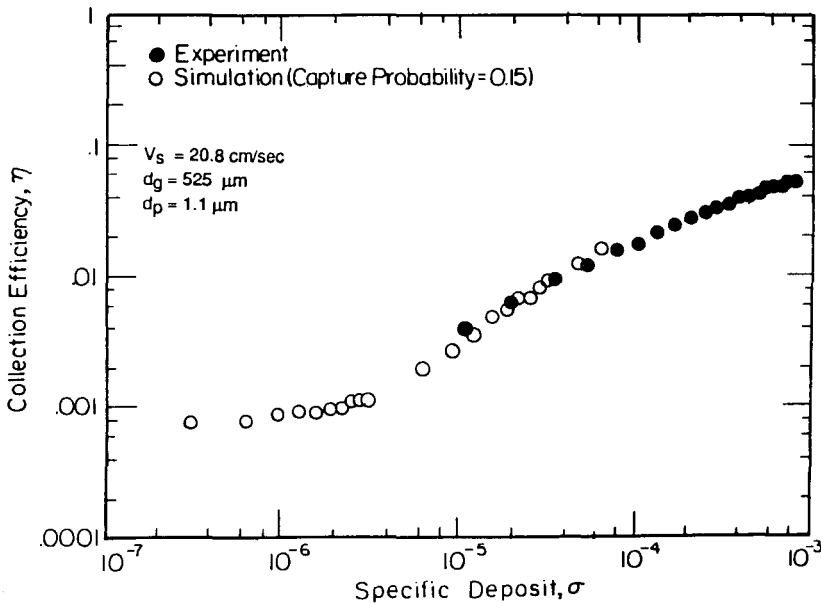


FIGURE 7. Agreement between simulation and experiment.

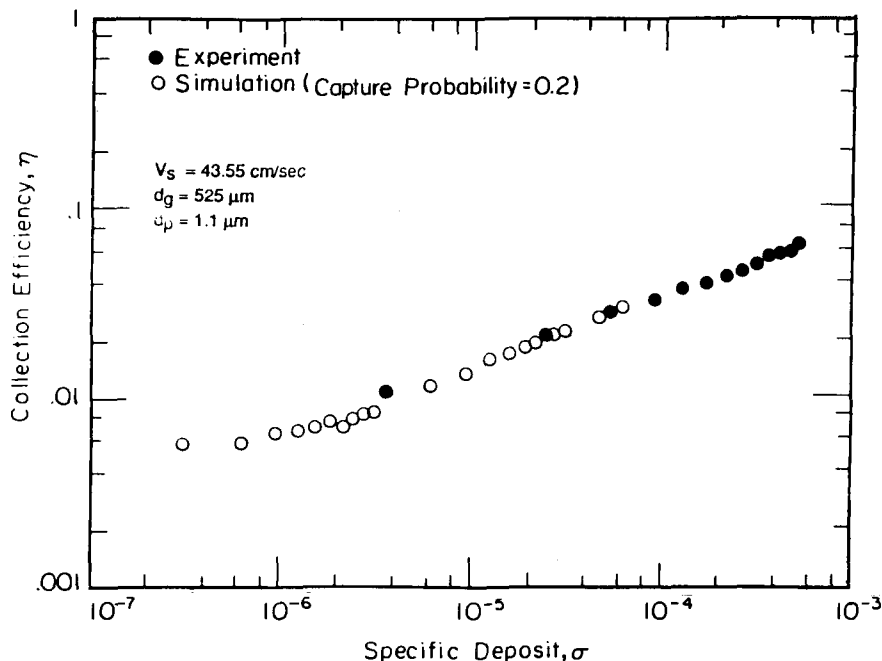


FIGURE 8. Agreement between simulation and experiment.

and collector size. A quantitative characterization of the deposit morphology and its evolution can be obtained by determining the size and size distribution of the particle clusters and their locations based on the average results of a number of simulations corresponding to the same set of conditions. An example is presented below.

Size of Particle Deposits. The sizes of particle clusters formed in particle deposition may be classified by grouping the cluster in the manner shown in Table 3. The number of particles belonging to each group of clusters at a given specific deposit can be counted in each simulation run. Therefore, from the ensemble average of these runs, one can determine the fractional contribution to deposition by particles in each group corresponding to a given specific deposit. An example of this representation is shown in Figure 9. It is clear that, as the extent of deposition

TABLE 3. Classification of Particle Clusters According to Size

Cluster type	Number of particles present in the cluster
1	1
2	2
3	3
4	4
5	5
6	6-10
7	11-20
8	21-40
9	41-60
10	61-100
11	101-200
12	201-400
13	401-600
14	601-800
15	801-1000
16	1001-1200
17	1201-1400
18	1401-1600
19	1601-1800
20	1801-2000
21	2001-2200
22	2201-2400

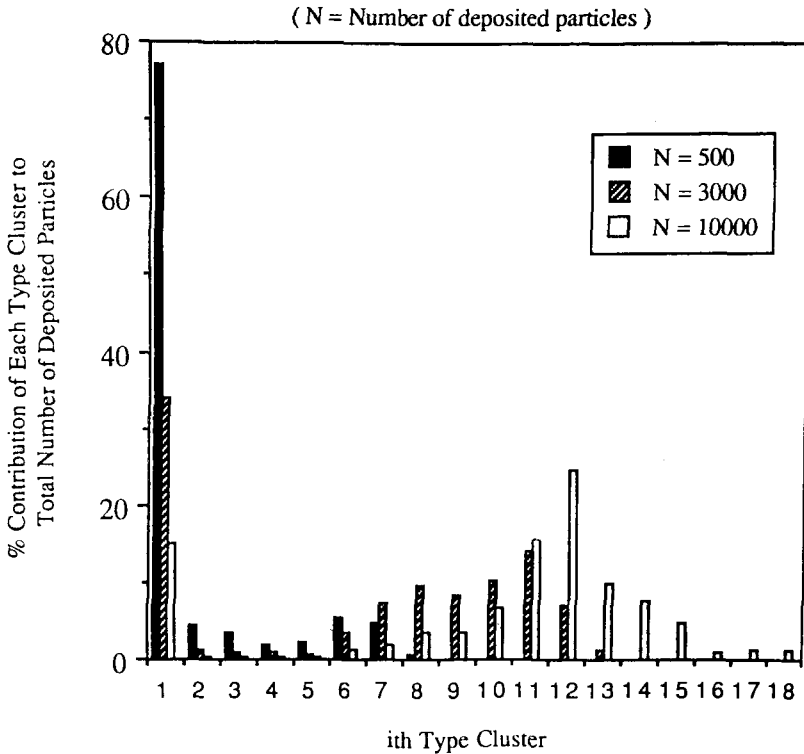


FIGURE 9. Particle cluster types and their numbers at various stages of deposition ($N_{St} = 3.605 \times 10^{-3}$, $N_R = 2.095 \times 10^{-3}$, $N_G = 2.14 \times 10^{-4}$).

becomes significant, particle deposition takes place mainly on the previously deposited particles, leading to the further growth of the existing particle clusters.

The effect of the Stokes number, N_{St} , on the morphology of particle deposition is shown in Figure 10. Figure 10 indicates that a greater N_{St} leads to a fewer but larger particle clusters. The effect of the interception parameter, N_R , shown in Figure 11 indicates that for the same number of deposited particles, a smaller N_R means a larger number of smaller dendrites. This behavior may be due to the fact that the probability of an incoming particle's making contact with any previously deposited particles is proportional to the size of the particles.

Positions of Particle Deposits. The morphology of particle deposits can also be analyzed in terms of their positions of deposition. To determine the deposition positions, the front half of the collector surface may be divided into a number of strips in the manner explained in Table 4. For example, a deposited particle with its θ coordinate falling within a given strip is considered to be deposited in the strip regardless of the value of its radial coordinate and azimuth angle. By counting the positions of deposition from simulation results, one can readily obtain the spatial distribution of particle deposition.

Concerning the effect of particle inertia (i.e., N_{St}) on the positions of particle deposition, Figure 12 shows that at larger

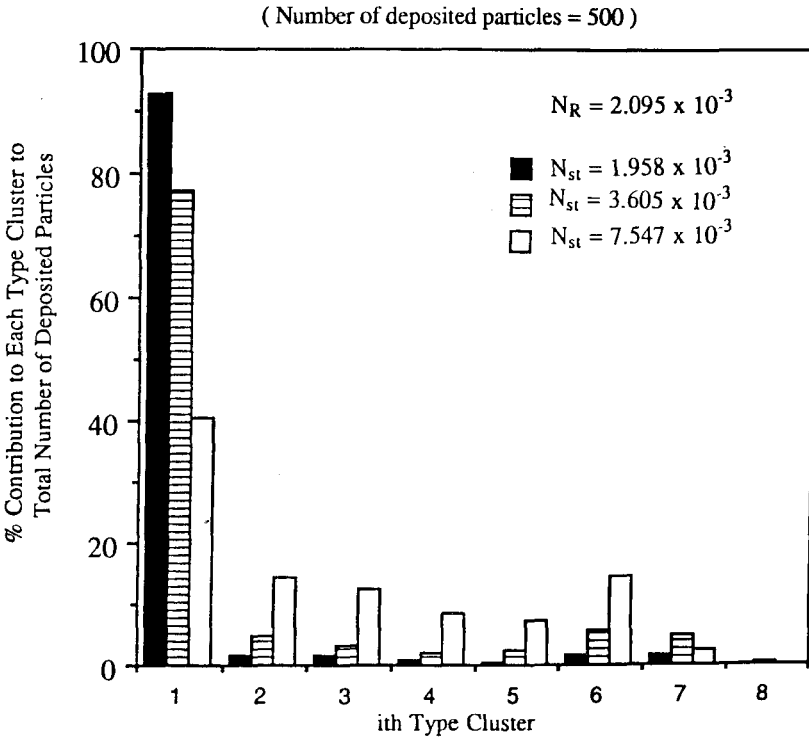


FIGURE 10. Effect of particle inertia on the size distribution of particle clusters.

N_{st} , particle deposition tends to take place mainly in the more immediate neighborhood of the stagnation point, a behavior which is not unexpected.

CONCLUSIONS

A simulation algorithm for the study of aerosol deposition in granular media was developed based on the use of a modified Happel model for characterizing the structure of the media. With the use of the algorithm and a super computer, particle deposition under conditions of practical extent can be simulated with reasonable computer time.

The concept of the capture probability was introduced to account for the various complications such as the change of the

flow field due to deposition, and the bounce-off of impacting particles which are not considered in the simulation. The value of the capture probability was determined empirically and its value was found to be insensitive to the operating condition. With the use of this correction factor, accurate prediction of the change in the unit collector efficiency with the extent of deposition can be simulated.

The simulation results make it possible to analyze the particle-deposit morphology in terms of the size and position of particle deposits. It was found that the two parameters, N_{st} and N_R , tend to give rise to few but large particle clusters, whereas larger N_{st} and N_R tend to result in many but small particle clusters. Therefore, one may expect that smaller parti-

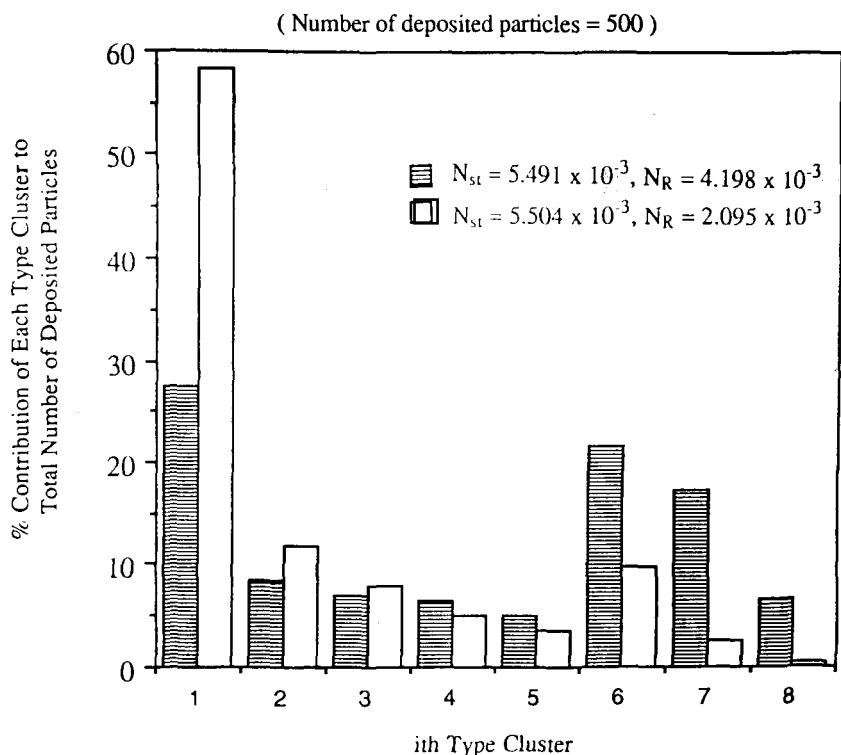


FIGURE 11. Effect of particle size on the size distribution of particle clusters.

TABLE 4. Classification of the Position of Particle Deposits in Terms of Their Angular Positions in θ Coordinate

ith strip	Angle from the axis of symmetry (degree)
1	0-3
2	3-6
3	6-9
4	9-12
5	12-15
6	15-18
7	18-21
8	21-24
9	24-27
10	27-30

cles are more likely to form large particle clusters than larger particles at the same specific deposit and gas velocity. Furthermore, particle clusters composed of small particles are expected to be more densely packed clusters made up of large particles. This means that the particle clusters made up of smaller particles are likely to be less permeable and to more effectively reduce the available pore space through which gas flows. As a result, it is expected that pressure drop across the filter bed as well as collection efficiency increases more significantly as filtration progresses. This qualitative trend has been found experimentally.

This study was performed under Grant NO. DE-FG02-88 ER 13930, Department of Energy, Office of Basic Energy Sciences.

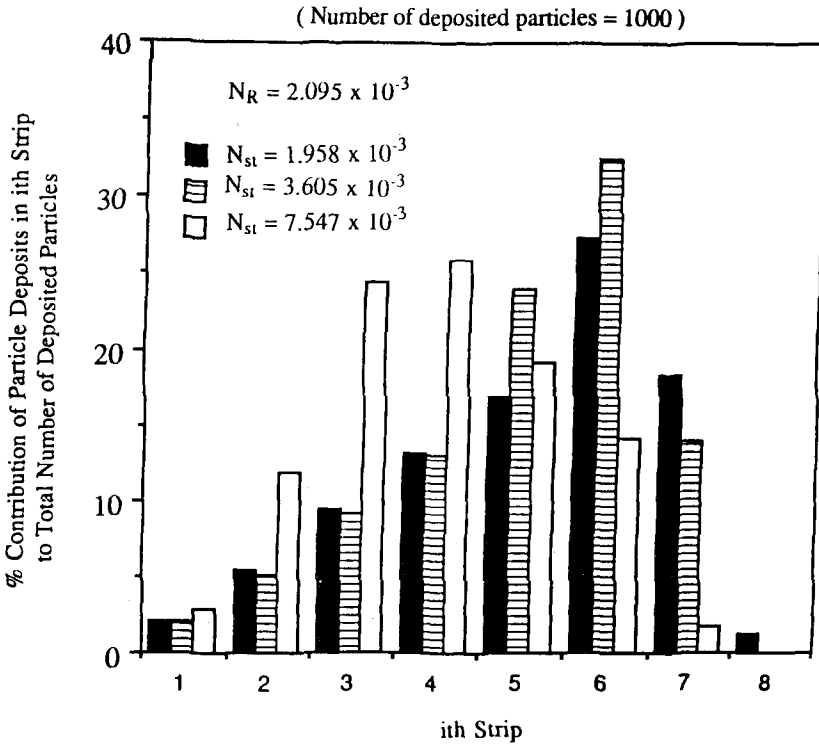


FIGURE 12. Effect of particle inertia on the positions of deposited particles.

APPENDIX

Expression for v_r and v_θ

A general solution for the axisymmetric creeping-flow equations in spherical coordinates is given by Happel and Brenner (1965):

$$\psi(r, \theta) = \sum_{n=2}^{\infty} [A_n r^n + B_n r^{n+1} + C_n r^{n+2} + D_n r^{n+3}] I_n(\mu) \tag{A1}$$

where

$$I_n(\mu) = \frac{P_{n-2}(\mu) - P_n(\mu)}{2n - 1}$$

and where ψ is stream function and

$P_n(\mu) = P_n(\cos \theta)$ is the Legendre polynomial of degree n .

The flow field in the modified Happel model are solved by determining the constants A_n , B_n , C_n , and D_n . The detailed procedure can be seen in Vaidyanathan's dissertation (1989).

The velocity fields v_r and v_θ are, therefore, obtained by the following relationships:

$$v_r = \frac{-1}{r^2 \sin \theta} \frac{\partial \psi}{\partial \theta} \tag{A2}$$

$$v_\theta = \frac{1}{r \sin \theta} \frac{\partial \psi}{\partial r} \tag{A3}$$

In this study, the maximum value of n was chosen as 50 and the values of the coefficients are listed in Table A1.

TABLE A1. Constants That Determine the Expression for ν_r and ν_θ

$\beta = 20^\circ, \varepsilon = 0.34$
For $n = 0, 1, 2, \dots, 50$

A_n	B_n	C_n	D_n
0.28160877114D + 03	0.80743418643D + 02	-.40040644616D + 02	-.32231154516D + 03
0.41540557612D + 02	0.50849812096D + 02	-.15143309124D + 02	-.77247060584D + 02
0.16126481968D + 02	0.34354890477D + 02	-.69480506143D + 01	-.43533321830D + 02
0.68347164122D + 01	0.20349818526D + 02	-.32101117538D + 01	-.23974423184D + 02
0.21593765369D + 01	0.79454126983D + 01	-.10957145122D + 01	-.90090747230D + 01
-.31696614766D + 00	-.15238183501D + 01	0.15689793047D + 00	0.16838865673D + 01
-.13393838129D + 01	-.67368474898D + 01	0.74114445716D + 00	0.73350868456D + 01
-.13595597047D + 01	-.75033365903D + 01	0.78775994369D + 00	0.80751363512D + 01
-.83414319704D + 00	-.49977585181D + 01	0.50089167046D + 00	0.53310100446D + 01
-.19219604799D + 00	-.12197884420D + 01	0.11978658696D + 00	0.12921979030D + 01
0.26874393844D + 00	0.19093099652D + 01	-.16743910571D + 00	-.20106147980D + 01
0.43674279598D + 00	0.32880368201D + 01	-.27824153572D + 00	-.34465380803D + 01
0.35910760256D + 00	0.28701864581D + 01	-.23246861979D + 00	-.29968254409D + 01
0.16397822219D + 00	0.13846778444D + 01	-.10766345614D + 00	-.14409926104D + 01
-.22234272864D - 01	-.20715508705D + 00	0.14458362358D - 01	0.21493099756D + 00
-.12606000320D + 00	-.11986927719D + 01	0.84004359548D - 01	0.12407484156D + 01
-.13687844623D + 00	-.13650583595D + 01	0.92044511730D - 01	0.14098922940D + 01
-.86849389423D - 01	-.90689535277D + 00	0.58856579783D - 01	0.93488816241D + 00
-.20758720603D - 01	-.22525180938D + 00	0.14198439804D - 01	0.23181209018D + 00
0.27627278678D - 01	0.31762115617D + 00	-.18886811973D - 01	-.32636162288D + 00
0.45292381579D - 01	0.54101398198D + 00	-.31164517397D - 01	-.55514184616D + 00
0.37168763843D - 01	0.46153588134D + 00	-.25704289242D - 01	-.47300035594D + 00
0.16937961960D - 01	0.21817584326D + 00	-.11770625582D - 01	-.22334317964D + 00
-.21625721394D - 02	-.29472892328D - 01	0.14965623611D - 02	0.30138902106D - 01
-.12674582389D - 01	-.17631572353D + 00	0.88565964106D - 02	0.18013370951D + 00
-.13704129338D - 01	-.19707341734D + 00	0.96113614417D - 02	0.20116618523D + 00
-.86528935247D - 02	-.12852493288D + 00	0.60888220031D - 02	0.13108900440D + 00
-.20718856261D - 02	-.31666846932D - 01	0.14639805349D - 02	0.32274752023D - 01
0.26944973949D - 02	0.42788618940D - 01	-.19034866760D - 02	-.43579629659D - 01
0.44097282931D - 02	0.72043386332D - 01	-.31248019969D - 02	-.73328312628D - 01
0.36041845635D - 02	0.60592970782D - 01	-.25603283791D - 02	-.61636826967D - 01
0.16374515230D - 02	0.28294725309D - 01	-.11660786595D - 02	-.28766098173D - 01
-.20323929364D - 03	-.36505090611D - 02	0.14440344089D - 03	0.37093449138D - 02
-.12076992835D - 02	-.22090896685D - 01	0.86253489877D - 03	0.22436061070D - 01
-.13020895173D - 02	-.24432491398D - 01	0.93180777753D - 03	0.24802773138D - 01
-.81971212250D - 03	-.15770227307D - 01	0.58768499762D - 03	0.16002254432D - 01
-.19635710999D - 03	-.38645410282D - 02	0.14110679519D - 03	0.39197913430D - 02
0.25231788788D - 03	0.51095778392D - 02	-.18129940143D - 03	-.51805963256D - 02
0.41241588626D - 03	0.85424848844D - 02	-.29686877954D - 03	-.86580319911D - 02
0.33626162551D - 03	0.71251274023D - 02	-.24240767547D - 03	-.72189813523D - 02
0.15248535208D - 03	0.33028280804D - 02	-.11008886825D - 03	-.33452245642D - 02
-.18623612786D - 04	-.41534779215D - 03	0.13426350451D - 04	0.42054505449D - 03
-.11151932205D - 03	-.25272407041D - 02	0.80656631684D - 04	0.25581033944D - 02
-.12001957491D - 03	-.27767917597D - 02	0.86913159655D - 04	0.28098981750D - 02
-.75415724076D - 04	-.17807330983D - 02	0.54676631088D - 04	0.18014721913D - 02
-.18067981638D - 04	-.43475542314D - 03	0.13119091969D - 04	0.43970431281D - 03
0.23047919880D - 04	0.56732887257D - 03	-.16733729586D - 04	-.57364306287D - 03
0.37639021742D - 04	0.94404259534D - 03	-.27359633082D - 04	-.95432198400D - 03
0.30640041400D - 04	0.78311589411D - 03	-.22293826676D - 04	-.79146210884D - 03
0.13877271395D - 04	0.36124030977D - 03	-.10107114701D - 04	-.36501033439D - 03

Downloaded by [IRSTEA] at 07:17 14 April 2015

REFERENCES

- Beizaie, M., Wang, C. S., and Tien, C. (1987). *Chem. Eng. Commun.* 13:153.
- Dahneke, B. E. (1972). *J. Colloid. Interface Sci.* 40:1.
- Gal, E., Tardos, G. I., and Pfeffer, R. (1985). *AIChE J.* 31:1093.
- Gupta, D., and Peters, M. H. (1985). *J. Colloid Interface Sci.* 104:375.
- Happel, J., and Brenner, H. (1965). *Low Reynolds Number Hydrodynamics*. Prentice-Hall Inc., Englewood Cliffs, NJ.
- Ho, C. P. (1981). *Collection of Solid Particles on Single Cylinders by Particle Inertia and Electrical Force*. Ph.D. Dissertation, Syracuse University, Syracuse, NY.
- Jung, Y. (1991). *Granular Filtration of Monodispersed and Polydispersed Aerosols*. Ph.D. Dissertation, Syracuse University, Syracuse, NY.
- Jung, Y., and Tien, C. (1991). *J. Aerosol Sci.* 22:187.
- Kanaoka, C., Emi, H., and Myojo, T. (1980). *J. Aerosol Sci.* 11:377.
- Paretsky, L., Theodore, L., Pfeffer, R., and Squires, A. M. (1971). *J. Aerosol Pollut. Contr. Assoc.* 21:204.
- Pendse, H., and Tien, C. (1982). *J. Colloid Interface Sci.* 87:225.
- Pendse, H., Turian, R. M., and Tien, C. *Deposition and Filtration of Particles from Gases and Liquids*. Society of Chemical Industry, London, p. 95.
- Press, W. H., Flannery, B. P., Teukolsky, S. A., and Vetterling, W. T. (1987). *Numerical Recipe*. Cambridge University Press, Cambridge.
- Ramarao, B. V., and Tien, C. (1988). *AIChE J.* 34:253.
- Snaddon, R. W. L., and Dietz, P. W. (1980). Report No. 80 CRD 290. General Electric Company, Schenectady, NY.
- Takahashi, T., Walata, S. A., and Tien, C. (1986). *AIChE J.*, 32:684.
- Tien, C. (1989). *Granular Filtration of Aerosols and Hydrosols*. Butterworths-Heinemann, Boston.
- Tien, C., Wang, C. S., and Barot, D. T. (1977). *Science* 196:983.
- Tsiang, R. C.-C. (1980). *Mechanics of Particle Deposition in Model Filters Composed of an Array of Parallel Fibers*. Ph.D. Dissertation, Syracuse University, Syracuse, NY.
- Tsiang, R. C.-C., Wang, C. S., and Tien, C. (1982). *Chem. Eng. Sci.* 37:1661.
- Ushiki, K., and Tien, C. (1985). *AIChE Sym. Ser.* 80:241:137.
- Vaidyanathan, R. (1989). *Colloid Deposition in Granular Media under Unfavorable Surface Conditions*. Ph.D. Dissertation, Syracuse University, Syracuse, NY.
- Vaidyanathan, R., Yao, C., and Tien, C. (1989). *Chin. Ind. Chem. Eng.* 20:209.
- Walata, S. A., Takahashi, T., and Tien, C. (1986). *Aerosol Sci. Technol.* 5:23.
- Wang, C. S., Beizaie, M., and Tien, C. (1977). *AIChE J.* 23:879.
- Yoshida, H., and Tien, C. (1985). *Aerosol Sci. Technol.* 4:360.
- Zener, C. (1941). *Phys. Rev.* 59:669.

Received June 10, 1992; accepted November 16, 1992